Efficient integrated module of gravity driven membrane filtration, solar aeration and GAC adsorption for pretreatment of shale gas wastewater

Gravity driven membrane filtration combined with solar aeration and GAC adsorption provides excellent productivity and effluent quality as shale gas wastewater pretreatment

Peng Tang[a,b], *Jialin Li*[a, b], *Lun Tian*[a, b], *Yu Sun*[a, b], *Wancen Xie*[a, b], *Qiping He*[c], *Haiqing Chang*[a, b], *Alberto Tiraferri*[d], *Baicang Liu*[a, b,*]

[a] Key Laboratory of Deep Earth Science and Engineering (Ministry of Education), College of Architecture and Environment, Institute of New Energy and Low-Carbon Technology, Sichuan University, Chengdu, 610207, PR China

[b] Yibin Institute of Industrial Technology, Sichuan University Yibin Park, Yibin, 644000, PR China

[c] Chuanqing Drilling Engineering Company Limited, Chinese National Petroleum Corporation, Chengdu 610081, PR China

[d] Department of Environment, Land and Infrastructure Engineering, Politecnico di Torino, Corso Duca degli Abruzzi 24, 10129 Turin, Italy

[*] Corresponding author.

Tel.: +86-28-85995998; fax: +86-28-62138325.

E-mail: bcliu@scu.edu.cn; baicangliu@gmail.com (B. Liu).

ABSTRACT

The rapid growth of shale gas extraction is associated to the increasing production of shale gas flowback and produced water: efficient treatment processes are urgently needed to allow better management of this wastewater. We propose a simple integrated pretreatment process for on-site treatment, whereby gravity driven membrane filtration is combined with granular activated carbon (GAC) adsorption and solar aeration. GAC and aeration significantly increased the stable flux and improved the final effluent quality of the membrane process. Specifically, the dissolved organic carbon removal rate of the integrated system was 44.9%, and the stable permeate flux was 1.7 times higher than that of simple gravity-driven filtration, which also showed negligible removal of organic. The high stable flux is attributed to a reduction of extracellular polymeric substances accumulated on the membrane, as well as to the more porous and heterogeneous biofilm formed thanks to the abundance and diversity of eukaryotes with active predation behavior. The prevailing strains, *Gammaproteobacteria* (35.5%) and *Alphaproteobacteria* (56.5%), played an important active role in organic carbon removal. The integrated system has great potential as pretreatment for shale gas flowback and produced water desalination due to its low energy consumption, low operational costs, high productivity, and effluent quality.

KEYWORDS: Shale gas flowback and produced water (SGFPW); Gravity driven membrane (GDM); Granular activated carbon (GAC); Aeration; Microbial community

Introduction

Shale gas may satisfy the current world's energy demand for over 60 years, and it is considered as a better resource to replace traditional fossil fuels and to help reducing the global carbon emissions (Chang et al., 2019a; Shaffer et al., 2013). However, the extraction of shale gas is presently associated with severe environmental problems, especially related to the great amount of freshwater that is consumed in the extraction activity and to the large flow of refractory shale gas flowback and produced water (SGFPW), with ~ 5200-25,870 m^3 generated per well (Chang et al., 2019b; Zou et al., 2018). SGFPW contains high concentrations of salinity, radionuclides, heavy metals, and refractory organics, seriously endangering human health, wildlife, and water ecosystems if not appropriately managed before discharge (Abass and Zhang, 2020; Butkovskyi et al., 2017). Furthermore, its quality and quantity change over time. For example, its salinity gradually increases, while the total organic carbon concentration reduces gradually with the life of the well (Barbot et al., 2013; Cluff et al., 2014). Shale gas extraction wells are often located in remote areas with scarce transportation and power facilities, making SGFPW treatment even more challenging.

Membrane technologies are considered the most appropriate and effective way to reuse SGFPW, achieving a sustainable cycle of water in the shale gas industry (Chang et al., 2019a; Tong et al., 2019). Desalination may by achieved by nanofiltration, reverse osmosis, forward osmosis, or membrane distillation. However, effective pretreatment is a significant factor in the sustainable operation of desalination (Chang et al., 2019c). Luckily, pretreatment can be effectively performed by low-pressure membrane processes, such as microfiltration (MF) and

ultrafiltration (UF) (Guo et al., 2018; Islam et al., 2019; Kim et al., 2018; Miller et al., 2013). Nevertheless, the appeal of such technologies is limited by the operational problems associated with membrane fouling (Chang et al., 2019c; Lee et al., 2019b). The recently developed gravity driven membrane filtration (GDM) is more favorable than conventional MF and UF in pretreating SGFPW (Chang et al., 2019c; Pronk et al., 2019). GDM has the advantages of simple operation, low maintenance, low energy consumption, and lower costs in general, mainly because its stable flux is realized by gravity and because the membrane does not need cleaning (Pronk et al., 2019). This technology has specific potential for the treatmeant of SGFPW generated from decentralized extraction wells.

In recent years, GDM technology has been successfully applied in many fields, such as in the treatment of surface water (Boulestreau et al., 2012; Chawla et al., 2017; Peter-Varbanets et al., 2010; Shao et al., 2019; Shi et al., 2020; Song et al., 2020a; Tang et al., 2018b; 2020b; Truttmann et al., 2020), rainwater (Ding et al., 2017b; Du et al., 2019; Wu et al., 2019), greywater (Ding et al., 2016; 2017a), sewage (Liu et al., 2020; Wang et al., 2017), and seawater (Akhondi et al., 2015; Wu et al., 2016; Wu et al., 2017). In our previous research (Chang et al., 2019c; Li et al., 2020), the suitability of the GDM process as a pretreatment option for SGFPW desalination was discussed, also assessing the long-term effects of operational parameters and analyzing the microbial community of the biofouling layer. While the performance was better than that of traditional UF, the GDM process still needs significant improvement. Chiefly, both the stable flux and the contaminant removal should be maximized to alleviate the fouling potential of the stream entering the desalination process.

In recent articles, the combination of GDM with other separation processes was discussed and broader conditions were evaluated, including the use of a biofilm reactor, adsorption, coagulation, and aeration (Ding et al., 2018b; Lee et al., 2019a; Lee et al., 2019b; Shao et al., 2017; Tang et al., 2018a; Tang et al., 2018b; Tang et al., 2018c). Specifically, granular activated carbon (GAC) has been reported to remarkably improve the permeate quality of GDM systems (Ding et al., 2018b; Lee et al., 2019b; Tang et al., 2018c). Regarding stable flux, Ding et al. (2018b) indicated that this was reduced because the GAC layer increased the filtration resistance. Lee et al. (2019b) attributed this effect to the lower presence, predation, and mobility of eukaryotes. In contrast, Tang et al. (2018c) found that GAC improved the diversity of eukaryotes with stronger predation ability in the biofouling layer, thus producing a more permeable biofouling layer. Additionally, Ding et al. (2016) analyzed the effect of aeration shear stress on a GDM system for greywater treatment. When the aeration was positioned below the membrane module, shear stress resulted in a thinner, denser, and less permeable biofouling layer with high EPS content, thus aggravating membrane fouling. Meanwhile, Peter-Varbanets et al. (2011) and Ding et al. (2017a) reported that high dissolved oxygen (7.9 mg/L, 6.0-6.5 mg/L) can promote high stable fluxes due to the enhanced biological activity, larger surface roughness, and lower EPS content in the biofouling layer. The effect of aeration on the GDM system is thus complex. On the one hand, aeration increases the dissolved oxygen level and the permeability of the biofouling layer. On the other hand, aeration shear stress might aggravate membrane fouling.

In this study, the effect of GAC and aeration on GDM performance is explored and

analyzed in the pretreatment of SGFPW . The specific objectives are to assess the effect of GAC and aeration on (1) stable flux, membrane fouling resistance, and permeate quality; (2) the morphology and accumulated biofoulants on the membrane; and (3) the diversity of bacterial and eukaryotic community present in the membrane biofilm. Therefore, an integrated system is proposed to improve the efficiency of SGFPW pretreatment for subsequent desalination.

Materials and methods

2.1 Gravity driven membrane filtration systems

A schematic diagram of the four GDM systems utilized in this work is shown in **Fig. 1.** The systems were operated in parallel at room temperature (~ 15℃) with hydrostatic pressure of 0.04 bar. The characteristics of the poly(vinylidene fluoride) hollow fiber UF membranes (Litree Purifying Technology Co., Ltd., China, with an effective membrane area of 15 cm^2) employed in this study can be found in previous reports (Li et al., 2020; Tang et al., 2020a). After 30 days of operation, the microbial environment tended to become stable. Then, No. 1 and No. 2 GDM units were aerated, and GAC was added to GDM units No. 1 and No. 3, to explore the effects of aeration and adsorption on the systems in the following 30 days of operation.

Specifically, a single crystal silicon solar air pump (Koge, Xiamen, China) continuously aerated No. 1 and No. 2 GDM units at a flow rate of 60 mL/min. To avoid direct erosion of membrane by aeration, thus aggravating membrane fouling effects (Ding et al., 2016), the aerators and the membrane modules were located on opposite sides of the reactors. The

concentration of dissolved oxygen measured by HQ30D dissolved oxygen analyzer (Hach Company, USA) was above 8 mg/L in aerated systems. In GDM units No. 1 and No. 3, 10 g GAC (CPG LF 12, Calgon Carbon Co., Ltd., USA) were added. GAC was cleaned with deionized water and dried before dosing. It was wrapped in gauze to prevent leakage, which might cause membrane fouling (Ding et al., 2018a; Ding et al., 2018b).

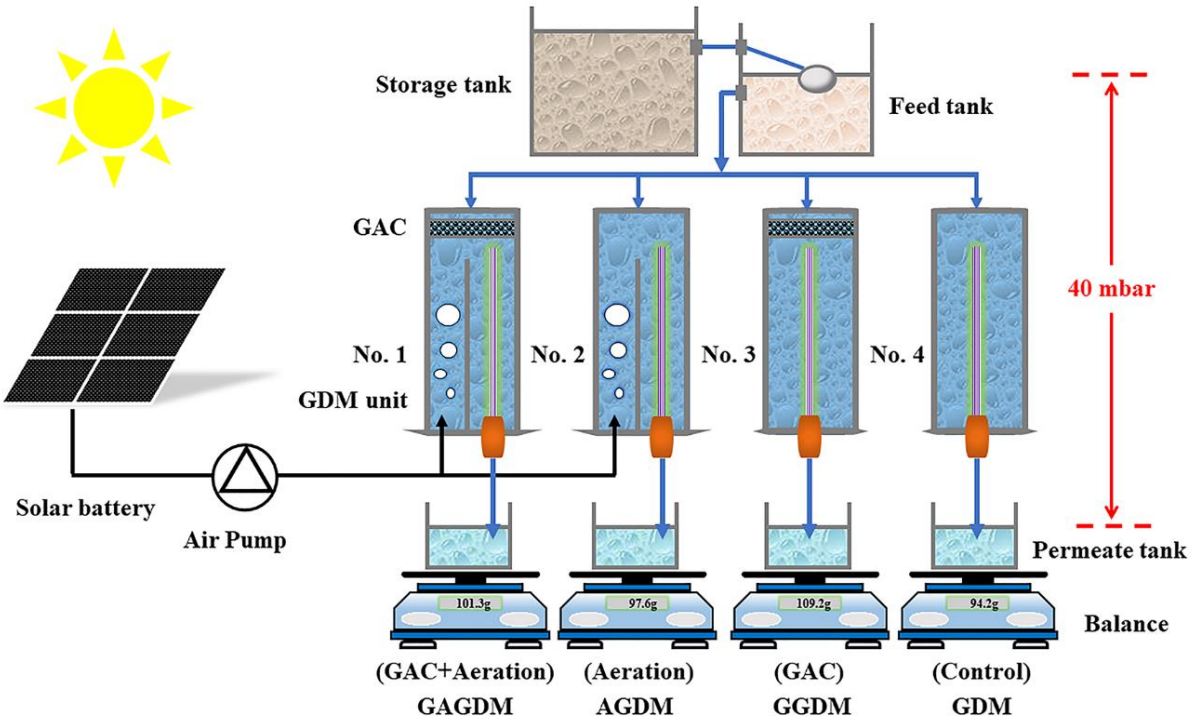

Fig. 1. Schematic diagram of the GDM systems. Four systems (GAGDM: GDM with GAC+aeration; AGDM: GDM with aeration only; GGDM: GDM with GAC only; GDM: control GDM) operated for a total of 60 days at room temperature (~ 15℃) with hydrostatic pressure of 0.04 bar.

2.2 Wastewater samples and water quality analysis

The shale gas flowback and produced water sample used in this study was collected from a drilling platform of the Weiyuan shale gas field in the Sichuan Basin, China. Compared to water

samples used in our previous research (Chang et al., 2019c; Li et al., 2020), the water samples utilized in this experiment were pale yellow and had a lower amount of suspended matters. The SGFPW samples were kept in sealed containers and in the dark to avoid changes in water quality. The pH value of the wastewater was measured using a pH meter (PB-10, Sartorius Scientific Instruments Co., Ltd., Beijing, China). The turbidity was determined by a HACH TL2310 turbidity meter (Hach, Loveland, CO, USA). The dissolved organic carbon (DOC) was determined with a TOC analyzer (TOC-L CPH, Shimadzu, Kyoto, Japan). The UV_{254} absorbance value was measured with a UV-vis spectrophotometer (Orion AquaMate 8000, Thermo Fisher Scientific Inc., MA, USA) at 254 nm wavelength. The concentration of total dissolved solids (TDS) and the electrical conductivity (EC) were determined using an Ultrameter II 6PFC portable multi-function apparatus (Myron L, Carlsbad, California, USA). The water quality characteristics of SGFPW samples are summarized in **Table 1**.

Table 1. Water quality characteristics of the SGFPW samples.

Constituents	SGFPW samples of Weiyuan shale gas field	
	This study	Previous literature (Chang et al., 2019c; Li et al., 2020; Shang et al., 2019; Tang et al., 2020a)
Turbidity (NTU)	35.9-42.7	32.5-215
pH	7.26-7.48	6.76-7.82
TDS (mg/L)	21,780-22,630	16,040-18,900
EC (mS/cm)	35.15-36.45	26.67-31.14
DOC (mg/L)	16.81-16.91	12.45-38.03
UV_{254} (cm^{-1})	0.162-0.173	0.057-0.165
DO (mg/L)	4.14-5.11	-

2.3 Membrane permeate flux and hydraulic resistance

The measurement and calculation methods of membrane permeate flux (L $m^{-2}h^{-1}$, LMH), total fouling resistance (R_t) and its components, *i.e.*, membrane inherent resistance (R_m), reversible resistance (R_{re}) and irreversible resistance (R_{ir}), were identical to our previous study (Chang et al., 2019d; Li et al., 2020).

2.4 Analysis of the membrane fouling layers

The EPS measuring method and details about the measurement of contact angle can be found in a recent study (Li et al., 2020). The surface of the fouled UF membrane samples were observed and analyzed by scanning electron microcopy (SEM) (FE-SEM, Regulus-8230, Hitachi, Japan) with energy dispersive spectroscopy (EDS) (X-MAX Extreme, Oxford-Instruments, UK) at an acceleration voltage of 15 kV. Before microscopy, dried membrane samples were sputter-coated with gold (MSP-2S, IXRF Systems Inc., USA).

2.5 Microbial diversity analysis

To explore the effects of aeration and GAC on microbial communities of GDM systems, part of the hollow fiber membranes (about 8 cm^2) were collected after filtration and quickly transferred to a sealed sterile tube. To prevent the decomposition of genetic material, the membrane samples were frozen with liquid nitrogen and stored in a refrigerator (906GP-ULTS, Thermo Scientific, USA) at −80℃. Details about DNA extraction, polymerase chain reaction (PCR) amplification, and Illumina Miseq sequencing are presented in **Text SI1** of the Supporting Information and in our previous study (Chang et al., 2019c). Briefly, for PCR amplification, the amplified primer sets of 18S rRNA genes for eukaryon and 16S rRNA

genes for bacteria were SSU0817/1196R and 338F/806R, respectively. UPARSE software (version 7.1 http://drive5.com/uparse/) was utilized to analyze the cluster operational taxonomic units (OTUs) with 97% similarity cutoff. The analysis of the alpha diversity, the beta diversity, and microbial community composition were performed with the Majorbio I-Sanger Cloud Platform (www.i-sanger.coom).

Results and discussion

4.1 Permeate flux and fouling resistance

The permeate flux profiles and the corresponding total fouling resistance of the four GDM systems observed during the 60 days of filtration are presented in **Figs. 2a** and **2b**. During the first 30 days, the systems were all equally run with no aeration and in the absence of GAC. In this period, the permeate flux decreased from 10.0 LMH to 2.53 LMH. Between the 30th to 40th day, the fluxes of all the systems decreased to values in the range 2-2.33 LMH at a slow rate, suggesting that GAC and aeration had negligible effect on flux decline. The GDM systems were backwashed on the 40th day to also analyze the effect of backwashing: to this purpose, some of the permeate was used as backwashing solution for ten minutes with 5 LMH back flux. Backwashing allowed recovery of a portion of permeate flux in all the systems. In particular, the flux of the control GDM system recovered only slightly from 2.28 LMH to 2.67 LMH (17% increase). The fluxes of AGDM, GGDM, and GAGDM units increased 26%, 80%, and 72%, respectively. This result suggests that the integrated features, especially the presence of GAC, improved the reversibility of membrane fouling.

After backwashing, normal operation was resumed for 20 more days and, at the end of the experiment, the fluxs of control GDM, AGDM, GGDM, and GAGDM systems were stable at values of 1.67, 1.87, 2.27, and 2.80 LMH, respectively. In this study, the stable fluxes were higher than those reported in our previous articles (Chang et al., 2019c; Li et al., 2020).

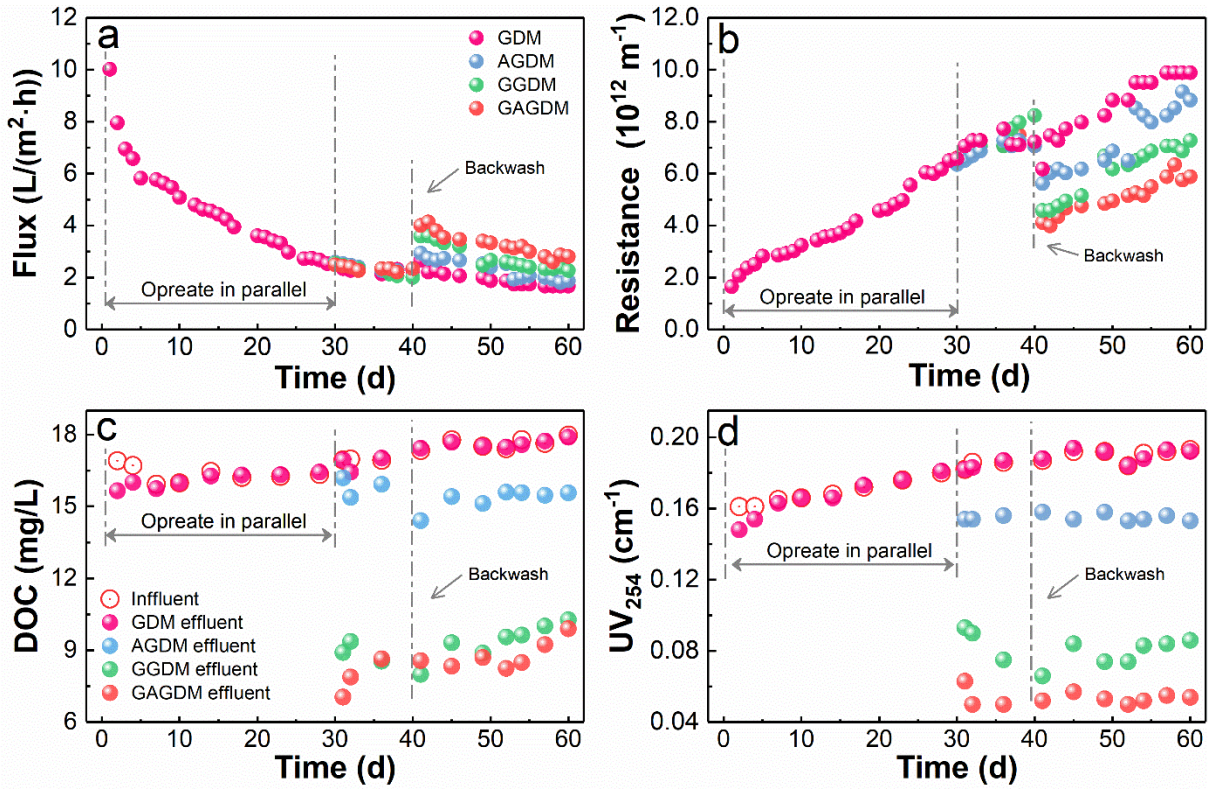

Fig. 2 The variation of (a) permeate flux, (b) total fouling resistance, (c) DOC of influent and effluent streams, and (d) UV_{254} of influent and effluent stream during the 60 days of filtration of the four GDM systems.

According to the flux results, the total fouling resistance of the filtration systems increased from about 1.64×10^{12} m^{-1} to about 6.51×10^{12} m^{-1} during the first 30 days of operation. Addition of GAC and of aeration diversified the evolution trends of total fouling resistance for the varioussystems. At the end of the experiment, the resistances in GDM,

AGDM, GGDM, and GAGDM units were 9.89×10^{12}, 8.83×10^{12}, 7.27×10^{12}, and 5.89×10^{12} m^{-1}, respectively. Overall, the performance was enhanced by aeration and was significantly improved by addition of GAC, for reasons that are discussed in the following sections.

4.2 Organic matter removal performance

Figs. 2c and **2d** present the removal efficiency of the filtration systems for DOC and UV_{254} during the 60 days of testing. At the beginning of the experiment, the DOC of the raw water was 16.9 mg/L, and the DOC in the effluent of control GDM system was 15.7 mg/L. Thus, the DOC removal rate was 7.5%. As the unit consists of a dead-end filtration reactor, the DOC of the feed solution was constantly increasing (Li et al., 2020; Wu et al., 2019). In the course of the filtration test, the DOC removal rate of the control GDM system was always negligible or even negative, because of the poor rejection combined with the effect of the biological layer on the membrane: macromolecular organic matter was likely degraded into smaller molecules by the biofilm, and passed more easily through the membrane pores compared to the starting material in the influent water (Akhondi et al., 2015; Derlon et al., 2016; Derlon et al., 2014; Peter-Varbanets et al., 2011; Tang et al., 2018c; Wu et al., 2019). A biofilm already formed on the membrane after short-term operation.

Upon addition of GAC and aeration, the DOC removal rate in AGDM, GGDM, and GAGDM units was 4.4%, 47.4%, and 58.4%, respectively, and stable during filtration. This sequence results in a DOC of the effluent equal to 17.9, 15.6, 10.3, and 9.90 mg/L, at the end of the tests. These observations indicate that aeration promoted DOC removal, probably because of the enhancement of microbial activity and the increase of the biomass

concentration in the two aerated reactors (Ding et al., 2017a; Lee et al., 2019a). Also, aeration seemed to improve the ability of GAC to adsorb organic matter, as already observed by previous studies (Karanfil et al., 1996; Lee et al., 2019a). For the two GDM systems provided with GAC, adsorption on activated carbon was the main reason for the high DOC removal rate in the initial period upon GAC addition; subsequently, the mechanism of DOC removal changed to slower bioadsorption and biodegradation (Lee et al., 2019b), as suggested also by previous investigations (Riley et al., 2016; Xing et al., 2008).

The UV_{254} removal efficiency was analogous to that of DOC. At the end of the filtration period, the UV_{254} of the effluents from control GDM, AGDM, GGDM, and GAGDM units was 0.192, 0.153, 0.086, and 0.054 cm^{-1}, respectively. Notably, aeration and especially GAC addition significantly improved the effluent water quality with great potential benefits for the subsequent desalination processes (Lee et al., 2019b).

4.3 Fouling reversibility and surface characteristics of membrane fouling layers

In order to investigate the effects of aeration and GAC on the recoverability of membrane fouling, we measured the pure water flux and pure water contact angle relative to the virgin membrane, the fouled membrane, and the fouled membrane after physical cleaning (Li et al., 2020); see the results summarized in **Fig. 3**.

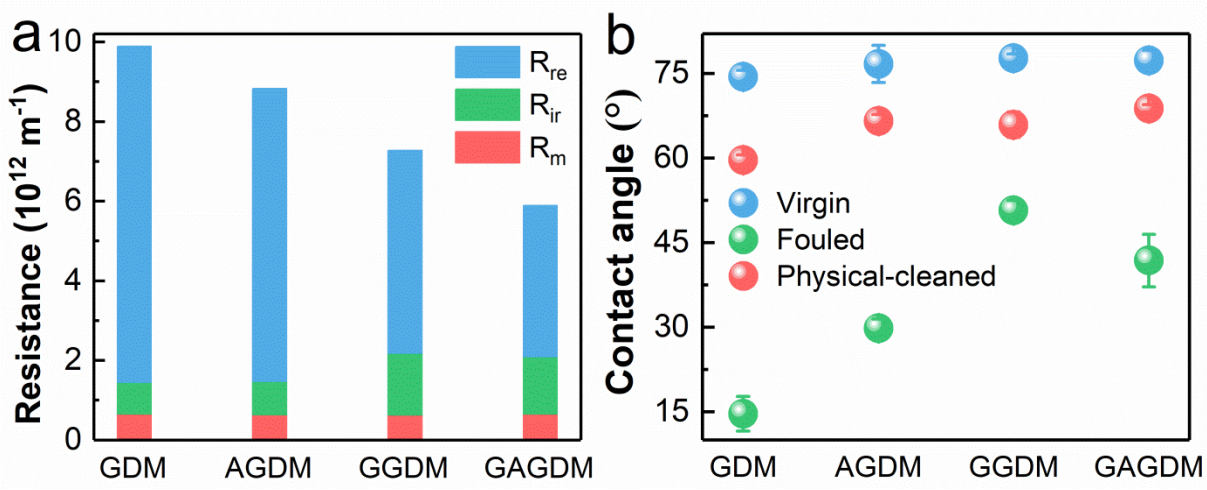

240

241 **Fig. 3** (**a**) Composition of membrane fouling resistance and (**b**) varation of water contact

242 angle on membranes from GDM systems with different operation conditions.

243

244 As shown in **Fig. 3a**, the total fouling resistance (R_t), reversible resistance (R_{re}) and

245 irreversible resistance (R_{ir}) of the control GDM system was 9.89×10^{12} m^{-1}, 8.45×10^{12} m^{-1},

246 and 0.79×10^{12} m^{-1}, respectively. R_{re} and R_{ir} accounted for 85.5% and 7.9% of R_t, in that order.

247 All the systems were characterized by a high reversibility resistance ratio (Chang et al., 2019c;

248 Ding et al., 2018b; Lee et al., 2019a). Compared with the R_t of the control system, the R_t of

249 the other filtration units was lower, with a reduction of 10.7%, 26.5% and 40.4%, respectively,

250 in AGDM, GGDM, and GAGDM systems. The trend of R_{re} was similar to that of R_t, whereas

251 R_{ir} increased for the systems in the presence of GAC, almost doubling in the GGDM unit.

252 This phenomenon suggests that GAC significantly reduced the R_{re}, which accounted for a

253 large proportion of the R_t, while increasing the R_{ir}, with aeration able to partly thwart this

254 effect. This phenomenon was not observed in previous research (Lee et al., 2019a; Tang et al.,

255 2018a; Tang et al., 2018c).

As shown in **Fig. 3b**, the water contact angles for all fouled membranes were markedly reduced, indicating the presence of hydrophilic foulants (Chang et al., 2019c). After physical cleaning, the contact angles recovered to values equivalent to roughly 80% of those measured with virgin membranes, which were in the range 75-77°. Similar to conclusions suggested by previous studies (Li et al., 2020; Wang et al., 2017), the pure water contact angle of the fouled membranes could be restored by physical cleaning to a level slightly lower than the original membrane, showing that the membrane fouling of GDM systems had high recoverability. The surface topographies of membrane fouling layers were observed with SEM and presented in **Fig. S1**. Compared to the sample employed in the control GDM unit, relatively loose and heterogeneous biofilm structures were found in the other three systems, in addition to many pores and cracks of different size.

4.4 Analysis of EPS on the fouling layer

The concentration of EPS on the membrane surface was measured at the end of the filtration tests. EPS was divided into loosely bound EPS (L-EPS) and tightly bound EPS (T-EPS), according to the different extraction methods (Li et al., 2020). The concentration of polysaccharide and protein was also measured, and all the results are presented in **Fig. 4**. The concentration of L-EPS and T-EPS in the membrane fouling layer of control GDM system was 1.68 and 0.42 g/m^2, respectively. The L-EPS consisted mostly of polysaccharides, while the fraction of protein represented about one third of the T-EPS.

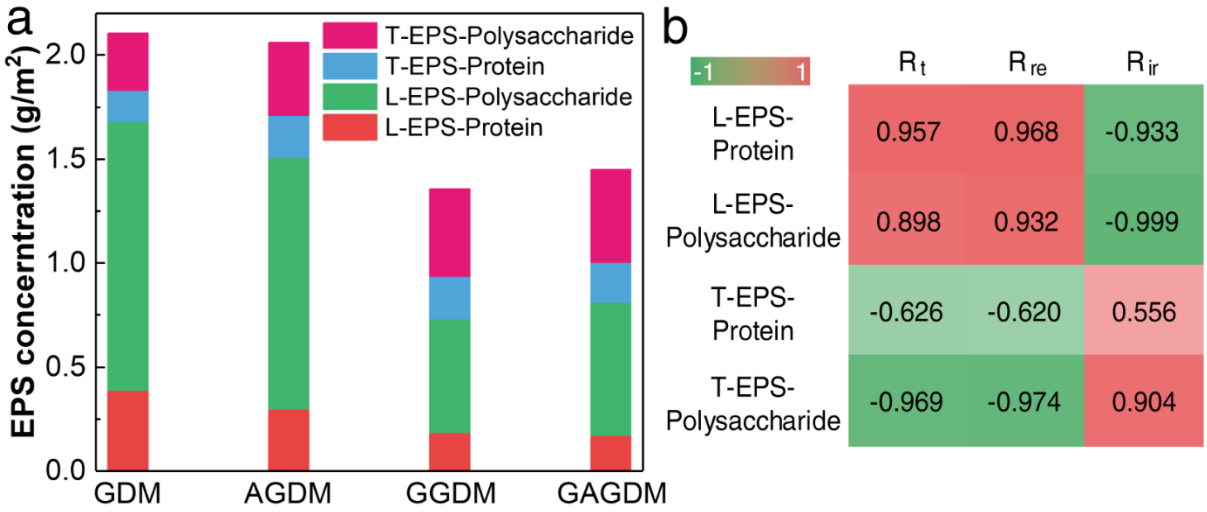

275

276 **Fig. 4** (**a**) The component of EPS accumulated on the membrane per unit area and (**b**) clustering

277 correlation analysis between EPS and membrane fouling resistance.

278

279 The effect of aeration on the concentration of L-EPS was not significant. However, it

280 seemed to lead to a certain increase in T-EPS concentration in the fouling layer, which might

281 be due to the shear force produced by aeration increasing the density of the layer (Pronk et al.,

282 2019). The concentrations of polysaccharide and protein in L-EPS is positively correlated

283 with R_t and R_{re}, as shown in **Fig. 4b**. GAC significantly reduced L-EPS concentration in the

284 membrane fouling layer, which might be the reason for the decrease of total fouling resistance

285 and of the reversible resistance. Similarly, some studies proposed that the reduction of EPS in

286 the biofouling layer is one of the main reasons for the increased stable flux in GDM (Tang et

287 al., 2018b; Tang et al., 2018c). In addition, the concentrations of polysaccharide in T-EPS is

288 positively correlated with R_{ir}. In fact, GAC increased the concentration of polysaccharide in

289 T-EPS, which might be the reason for the increase in the irreversible resistance in systems

290 comprising activated carbon (Fig. 3a).

4.5 Microbial diversity analysis

The Venn diagram of bacterial and eukaryotic communities at OTU level and the alpha diversity of bacterial and eukaryotic communities are shown in **Fig. 5**. Overall, the diversity and richness of microorganisms in this work was higher than in samples analyzed in our previous research (Chang et al., 2019c), and than in other samples from the Sichuan basin (Zhang et al., 2017). However, it was far lower than that of waste sludge, soil, or wastewater samples, due to the harsh water quality characterics of SGFPW (Wang et al., 2019). The coverage values of all samples were higher than 99.9% (**Figs. 5b** and **5d**), indicating that the sequencing depth was sufficient to cover most of bacteria and eukaryotes. The rarefaction curves (**Fig. S2**) also suggest that the sequencing depth was adequate.

In terms of bacterial communities, a total of 378 OTUs were found across all samples with a range of 269-323 OTUs present in each sample. The highest OTU number was found for the biolayer evolved in the control GDM system. The number of OTUs from GGDM and GAGDM units was close and sightly lower than that of the control system, indicating that the addition of GAC and aeration only affected a small portion of the bacteria in the fouling layer. The decrease in ACE index and Shannon index also indicated that GAC and aeration slightly reduced the richness and diversity of the bacterial communitiy.

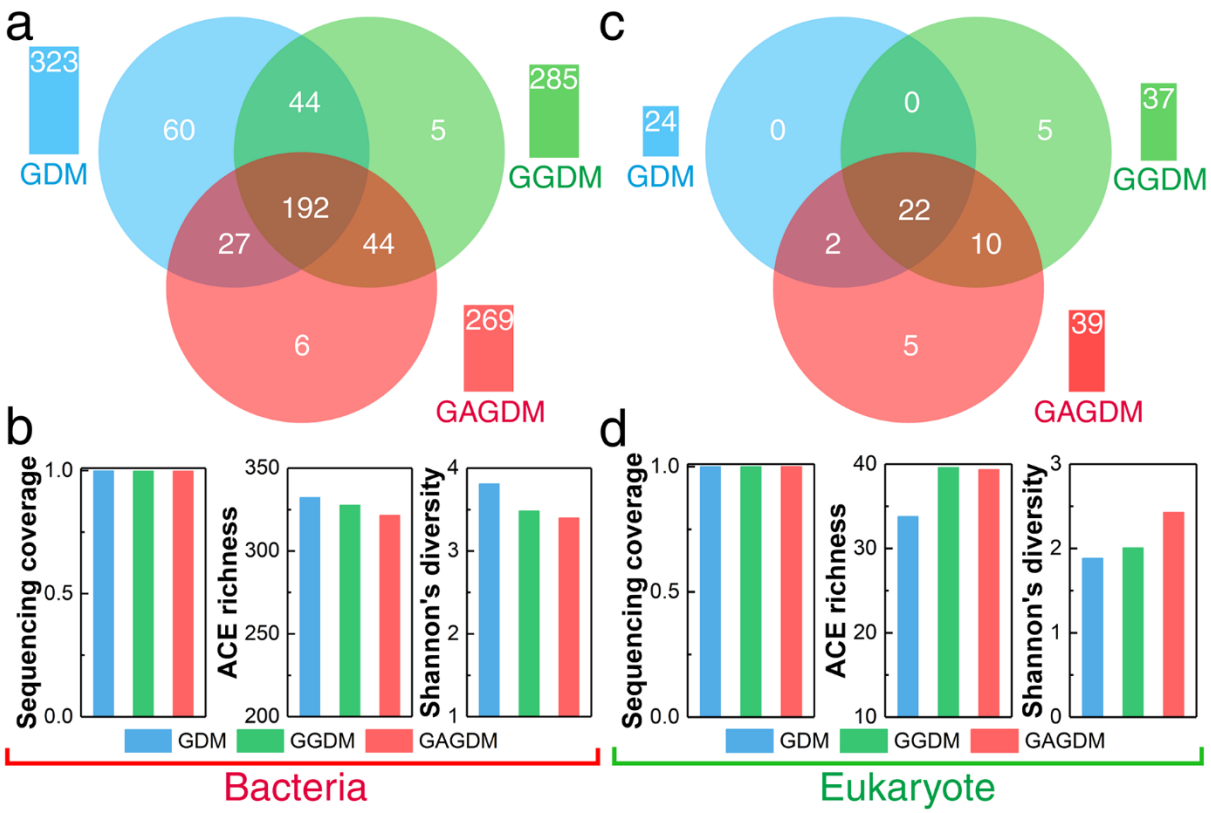

Fig. 5 Venn diagram of bacterial (**a**) and eukaryotic (**c**) communities and the alpha diversity of bacterial (**b**) and eukaryotic (**d**) communities.

The richness and diversity of eukaryotic communities were much smaller than those relative to bacteria, but opposite trends were observed upon combination of the GDM system with GAC and aeration. A total of 44 OTUs were detected in the eukaryotic community of biolayer from three GDM systems. The control group did not have a unique OTU, while a large number of new OTUs were detected in the biofilm from the GGDM and GAGDM units. The variation of ACE index and Shannon index indicated that addition of GAC enriched the richness and diversity of the eukaryotic community in the membrane fouling layer, while aeration had only a small further enhancing effect.

4.5.1 Bacterial community of the biofouling layer in GDM systems

There were 30 kinds of bacterial phyla in the membrane biofouling layer of three GDM systems; see **Fig. 6a**. *Proteobacteria* (50.3%), *Tenericutes* (13.1%), *Epsilonbacteraeota* (8.6%), *Bacteroidetes* (4.2%), and *Firmicutes* (4.3%) were the major phyla and constituted 80.5% of the bacteria in the control GDM system. Some halotolerant and halophilic bacteria existed in phyla *Proteobacteria and Bacteroidetes* (Frank et al., 2017; Zhang et al., 2017). Consistent with what discussed above, GAC and combined GAC with aeration significantly decreased the diversity of the bacterial community and changed the community structure at the phylum level. In particular, the vast majority of the phyla was represented by *Proteobacteria* in samples from GGDM and GAGDM units (> 90%). The existence of *Proteobacteria* is common to wastewater because of their ability to decompose carbohydrates (Frank et al., 2017; Song et al., 2020b).

Alphaproteobacteria (39.8%), *Mollicutes* (13.1%), *Campylobacteria* (8.5%), *Deltaproteobacteria* (6.1%), *Clostridia* (4.3%) and *Gammaproteobacteria* (4.2%) were the main classes found in the biofilm from the control GDM system. In GGDM and GAGDM samples, *Alphaproteobacteria* and *Gammaproteobacteria* affiliated to *Proteobacteria* increased, especially *Gammaproteobacteria*, as shown in **Fig. 6b**. According to reports, halophilic bacteria of these two classes can effectively degrade polycyclic aromatic hydrocarbons in polluted seawater (Arulazhagan and Vasudevan, 2009). The *Gammaproteobacteria* and *Alphaproteobacteria* might also play an important role in high DOC removal. In the biolayer evolved in the GAGDM system, the relative abundance of *Deltaproteobacteria* was obviously reduced to 0.8%: this result is not surprising because the dominant organisms of this class have anaerobic metabolism function, including

sulfate-reducing bacteria and geobacter sub-phylum (Freedman et al., 2017).

At the genus level, 231 bacteria genuses were detected in the samples from the three systems. The core genuses from the control GDM unit were *unclassified_o_Rhizobiales* (21.7%), *norank_f_Izimaplasmataceae* (12.9%), *Parvibaculum* (8.6%), *Sulfurospirillum* (7.8%), *Hyphomonas* (3.7%), and *Desulfuromonas* (2.8%). GAC and combined GAC with aeration significantly changed the core genuses, which for GGDM and GAGDM samples were *Denitromonas* (18.3-21.5%), *Thalassospira* (6.2-14.0%), *Labrenzia* (3.5-9.6%), *Marinobacter* (6.1-8.1%), *Hyphomonas* (7.6-9.7%), *Parvibaculum* (2.0-6.2%), *unclassified_o_Rhizobiales* (3.3-5.9%), and *Roseovarius* (1.6-2.3%), significantly different with those extracted from the membrane used in the control GDM system.

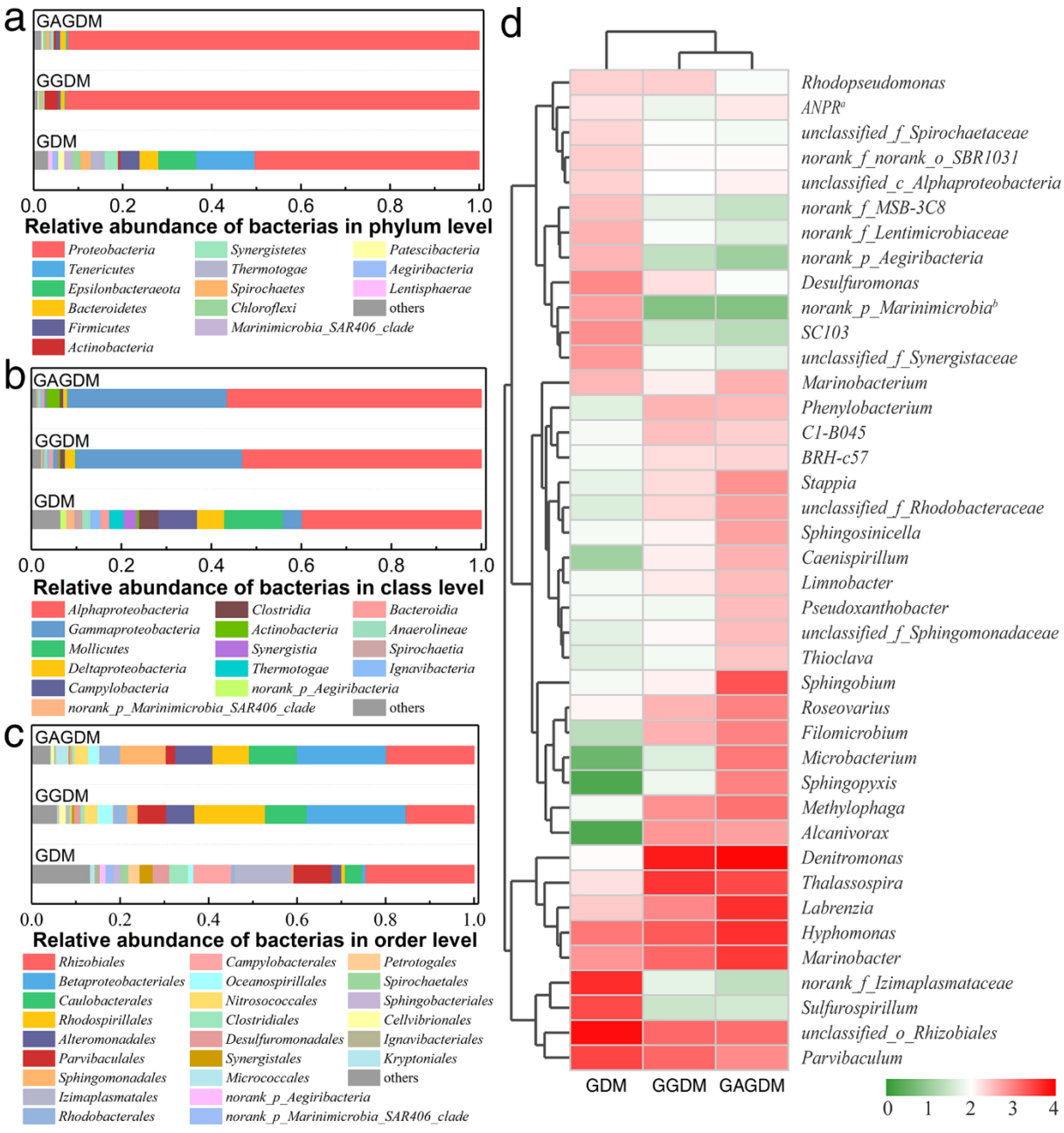

Fig. 6 Bacterial community compositions at (a) the phylum (>0.5%), (b) the class (>1%), (c) the order (>1%), and (d) the genus level (top 40). In (d), ANPR[a] and norank_p_Marinimicrobia[b] represent Allorhizobium-Neorhizobium-Pararhizobium-Rhizobium and norank_p_Marinimicrobia_SAR406_clade, respectively.

4.5.2 Eukaryotic community of the biofouling layer in GDM systems

360 **Fig. 7a** shows that the eukaryotic kingdom of the biofilm from the control GDM system
361 consisted of *Fungi* (79.9%), *Excavata* (20.0%), and *Alveolata* (0.1%), which was a different
362 classification compared to our previous study (Chang et al., 2019c). The fraction of *Fungi*
363 increased significantly to 95.7-99.8% in GGDM and GAGDM samples, representing the
364 vastly predominant eukaryotic kingdom. At the phylum level, *Ascomycota* (72.4-87.7%) and
365 *Basidiomycota* (7.5-16.5%) were dominant in all systems, and a similar observation was
366 reported in other SGFPW samples from the Sichuan Basin (Zhang et al., 2017). The number
367 of classes observed in GDM, GGDM, and GAGDM samples was 7, 17, and 16, respectively.
368 Finally, as shown in **Fig. 7e**, the core genera of the biofilm evolved in the control GDM system
369 were *Cladosporium* (46.3%), *Trimastix* (20.0%), *unclassified_f_Aspergillaceae* (9.2%),
370 *Fusarium* (7.8%) and *unclassified_o_Saccharomycetales* (7.7%). The *Cladosporium* fungi can
371 produce extracellular hydrolytic enzymes, like monoacyl esterase, protease, and pectinolytic
372 enzymes (Barbosa et al., 2001). Addition of GAC and combined GAC with aeration changed
373 the environment significantly, thus modifying the core genera. Specifically, the fouling layer
374 environment of the latter unit was beneficial to the growth of *Fusarium* (31.8-44.0%),
375 *norank_f__Cucurbitariaceae* (6.5-10.4%), and *Boeremia* (6.2-8.9%). In contrast, it was
376 detrimental to the growth of *Cladosporium* (17.4-19.2%), *Trimastix* (0.1-0.5%),
377 *unclassified_f_Aspergillaceae* (3.4-5.0%) and *unclassified_o_Saccharomycetales* (0.02-0.1%).
378 Overall, the clear increase in abundance and diversity of eukaryotes by GAC and aeration
379 should be accompanied by more active predation behavior, resulting in a more porous and
380 heterogeneous membrane biofouling layer, thereby increasing the stable flux of the filtration

system (Chang et al., 2019c; Pronk et al., 2019; Tang et al., 2018a; Tang et al., 2018c).

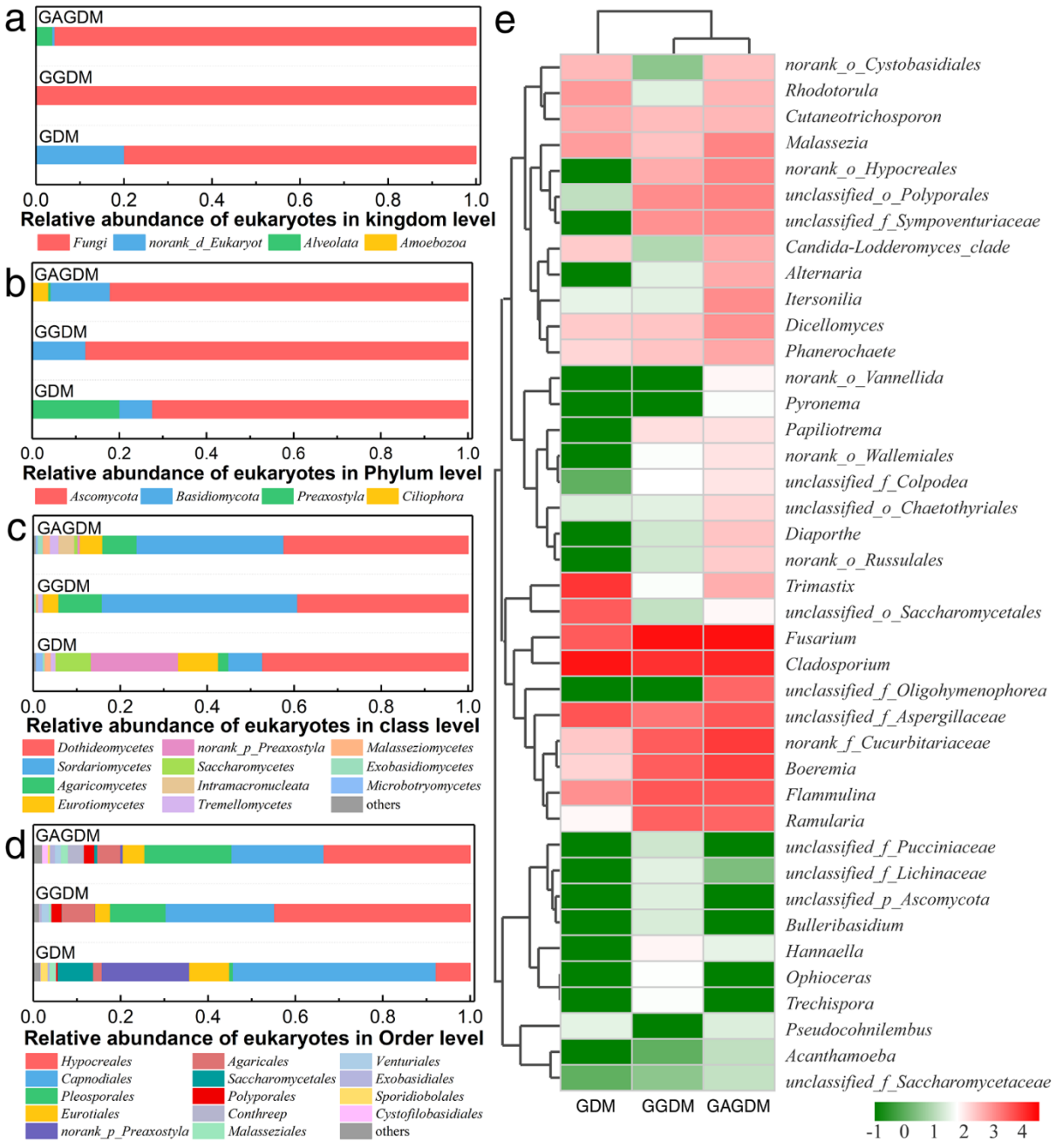

Fig. 7 Eukaryotic community compositions at (**a**) the kingdom, (**b**) the phylum, (**c**) the class (>1%), (**d**) the order (>1%), and (**e**) the genus level.

Conclusions

To solve the issue about low stable flux and low organic removal of gravity driven

membrane filtration, solar aeration and in-situ GAC adsorption were combined with GDM to pretreat SGFPW in Weiyuan. The performance of the integrated processes and the characteristics of the membrane fouling layers obtained under different conditions were evaluated and the following conclusions can be drawn:

(1) GAC and aeration, especially GAC, markedly enhanced the stable flux and reduced the total fouling resistance of GDM systems. GAC significantly reduced R_{re}, which accounted for a large proportion of R_t and it also slightly increased the R_{ir} of GDM systems. Aeration can further reduce R_t of the GDM system when combined with GAC.

(2) Compared to traditional units, the system comprising both GAC adsorption and aeration showed high DOC removal rate due to bioabsorption and biodegradation. GAC significantly reduced the concentration of EPS in the membrane biofouling layer and this effect is one of the main reasons for the increased stable flux of the integrated system.

(3) GAC and aeration observably changed the the microbial community structure. The dominant *Gammaproteobacteria* (35.5%) and *Alphaproteobacteria* (56.5%) classes evolved in the GAGDM integrated system played an important role in high DOC removal. In this unit, the eukaryotic community richness and diversity significantly increased in the biofouling layer. This is accompanied with more active predation behavior, resulting in a more porous and heterogeneous membrane biofouling layer, thus translating into a higher system productivity.

Acknowledgments

This work was supported by the National Natural Science Foundation of China (51678377, 51708371), and Sichuan University and Yibin City People's Government strategic

cooperation project (2019CDYB-25). We would like to thank the Institute of New Energy and Low-Carbon Technology, Sichuan University, for SEM-EDS measurement.

Appendix A. Supplementary data

The Supporting Information to this article is available at online. Detailed experimental procedures and additional experimental data: DNA extraction, polymerase chain reaction (PCR) amplification, and Illumina Miseq sequencing; SEM images and EDS analyses of membrane fouling layers in different GDM systems; Rarefaction curves of OTUs for bacteria and eukaryote in biofouling layers of three GDM systems.

References

Abass, O.K. and Zhang, K. 2020. Nano-Fe mediated treatment of real hydraulic fracturing flowback and its practical implication on membrane fouling in tandem anaerobic-oxic membrane bioreactor. J. Hazard. Mater. 395, 122666. https://doi.org/10.1016/j.jhazmat.2020.122666

Akhondi, E., Wu, B., Sun, S.Y., Marxer, B., Lim, W.K., Gu, J., Liu, L.B., Burkhardt, M., McDougald, D., Pronk, W. and Fane, A.G. 2015. Gravity-driven membrane filtration as pretreatment for seawater reverse osmosis: Linking biofouling layer morphology with flux stabilization. Water Res. 70, 158-173. https://doi.org/10.1016/j.watres.2014.12.001

Arulazhagan, P. and Vasudevan, N. 2009. Role of a moderately halophilic bacterial consortium in the biodegradation of polyaromatic hydrocarbons. Mar. Pollut. Bull. 58(2), 256-262. https://doi.org/10.1016/j.marpolbul.2008.09.017

Barbosa, M.A.G., Rehn, K.G., Menezes, M. and Mariano, R.d.L.R. 2001. Antagonism of Trichoderma species on Cladosporium herbarum and their enzimatic characterization. Braz. J. Microbiol. 32, 98-104. https://doi.org/10.1590/S1517-83822001000200005

Barbot, E., Vidic, N.S., Gregory, K.B. and Vidic, R.D. 2013. Spatial and Temporal Correlation of Water Quality Parameters of Produced Waters from Devonian-Age Shale following Hydraulic Fracturing. Environ. Sci. Technol. 47(6), 2562-2569. https://doi.org/10.1021/es304638h

Boulestreau, M., Hoa, E., Peter-Verbanets, M., Pronk, W., Rajagopaul, R. and Lesjean, B. 2012. Operation of gravity-driven ultrafiltration prototype for decentralised water supply. Desalin. Water Treat. 42(1-3), 125-130. https://doi.org/10.1080/19443994.2012.683073

Butkovskyi, A., Bruning, H., Kools, S.A.E., Rijnaarts, H.H.M. and Van Wezel, A.P. 2017. Organic pollutants in shale gas flowback and produced waters: Identification, potential ecological impact, and implications for treatment strategies. Environ. Sci. Technol. 51(9), 4740-4754. https://doi.org/10.1021/acs.est.6b05640

Chang, H., Li, T., Liu, B., Vidic, R.D., Elimelech, M. and Crittenden, J.C. 2019a. Potential and implemented membrane-based technologies for the treatment and reuse of flowback and produced water from shale gas and oil plays: A review. Desalination 455, 34-57. https://doi.org/10.1016/j.desal.2019.01.001

Chang, H., Liu, B., Crittenden, J.C. and Vidic, R.D. 2019b. Resource Recovery and Reuse for Hydraulic Fracturing Wastewater in Unconventional Shale Gas and Oil Extraction. Environ. Sci. Technol. 53(23), 13547-13548. https://doi.org/10.1021/acs.est.9b06240

Chang, H., Liu, B., Wang, H., Zhang, S.Y., Chen, S., Tiraferri, A. and Tang, Y.Q. 2019c. Evaluating the performance of gravity-driven membrane filtration as desalination pretreatment of shale gas flowback and produced water. J. Membr. Sci. 587, 117187. https://doi.org/10.1016/j.memsci.2019.117187

Chawla, C., Zwijnenburg, A., Kemperman, A.J.B. and Nijmeijer, K. 2017. Fouling in gravity driven Point-of-Use drinking water treatment systems. Chem. Eng. J. 319, 89-97. https://doi.org/10.1016/j.cej.2017.02.120

Cluff, M.A., Hartsock, A., MacRae, J.D., Carter, K. and Mouser, P.J. 2014. Temporal Changes in Microbial Ecology and Geochemistry in Produced Water from Hydraulically

Fractured Marcellus Shale Gas Wells. Environ. Sci. Technol. 48(11), 6508-6517. https://doi.org/10.1021/es501173p

Derlon, N., Grutter, A., Brandenberger, F., Sutter, A., Kuhlicke, U., Neu, T.R. and Morgenroth, E. 2016. The composition and compression of biofilms developed on ultrafiltration membranes determine hydraulic biofilm resistance. Water Res. 102, 63-72. https://doi.org/10.1016/j.watres.2016.06.019

Derlon, N., Mimoso, J., Klein, T., Koetzsch, S. and Morgenroth, E. 2014. Presence of biofilms on ultrafiltration membrane surfaces increases the quality of permeate produced during ultra-low pressure gravity-driven membrane filtration. Water Res. 60, 164-173. https://doi.org/10.1016/j.watres.2014.04.045

Ding, A., Liang, H., Li, G., Derlon, N., Szivak, I., Morgenroth, E. and Pronk, W. 2016. Impact of aeration shear stress on permeate flux and fouling layer properties in a low pressure membrane bioreactor for the treatment of grey water. J. Membr. Sci. 510, 382-390. https://doi.org/10.1016/j.memsci.2016.03.025

Ding, A., Liang, H., Li, G.B., Szivak, I., Traber, J. and Pronk, W. 2017a. A low energy gravity-driven membrane bioreactor system for grey water treatment: Permeability and removal performance of organics. J. Membr. Sci. 542, 408-417. https://doi.org/10.1016/j.memsci.2017.08.037

Ding, A., Wang, J.L., Lin, D.C., Cheng, X.X., Wang, H., Bai, L.M., Ren, N.Q., Li, G.B. and Liang, H. 2018a. Effect of PAC particle layer on the performance of gravity-driven membrane filtration (GDM) system during rainwater treatment. Environ. Sci. Water Res. Technol. 4(1), 48-57. https://doi.org/10.1039/c7ew00298j

Ding, A., Wang, J.L., Lin, D.C., Tang, X.B., Cheng, X.X., Wang, H., Bai, L.M., Li, G.B. and Liang, H. 2017b. A low pressure gravity-driven membrane filtration (GDM) system for rainwater recycling: Flux stabilization and removal performance. Chemosphere 172, 21-28. https://doi.org/10.1016/j.chemosphere.2016.12.111

Ding, A., Wang, J.L., Lin, D.C., Zeng, R., Yu, S.P., Gan, Z.D., Ren, N.Q., Li, G.B. and Liang, H. 2018b. Effects of GAC layer on the performance of gravity-driven membrane filtration (GDM) system for rainwater recycling. Chemosphere 191, 253-261. https://doi.org/10.1016/j.chemosphere.2017.10.034

Du, X., Xu, J.J., Mo, Z.Y., Luo, Y.L., Su, J.H., Nie, J.X., Wang, Z.H., Liu, L.F. and Liang, H. 2019. The performance of gravity-driven membrane (GDM) filtration for roofing rainwater reuse: Implications of roofing rainwater energy and rainwater purification. Sci. Total Environ. 697. https://doi.org/10.1016/j.scitotenv.2019.134187

Frank, V.B., Regnery, J., Chan, K.E., Ramey, D.F., Spear, J.R. and Cath, T.Y. 2017. Co-treatment of residential and oil and gas production wastewater with a hybrid sequencing batch reactor-membrane bioreactor process. J. Water Process Eng. 17, 82-94. https://doi.org/10.1016/j.jwpe.2017.03.003

Freedman, D.E., Riley, S.M., Jones, Z.L., Rosenblum, J.S., Sharp, J.O., Spear, J.R. and Cath, T.Y. 2017. Biologically active filtration for fracturing flowback and produced water treatment. J. Water Process Eng. 18, 29-40. https://doi.org/10.1016/j.jwpe.2017.05.008

Guo, C., Chang, H., Liu, B., He, Q., Xiong, B., Kumar, M. and Zydney, A.L. 2018. A

combined ultrafiltration–reverse osmosis process for external reuse of Weiyuan shale gas flowback and produced water. Environ. Sci. Water Res. Technol. 4(7), 942-955. https://doi.org/10.1039/C8EW00036K

Islam, M.S., Touati, K. and Rahaman, M.S. 2019. Feasibility of a hybrid membrane-based process (MF-FO-MD) for fracking wastewater treatment. Sep. Purif. Technol. 229, 115802. https://doi.org/10.1016/j.seppur.2019.115802

Karanfil, T., Schlautman, M.A., Kilduff, J.E. and Weber, W.J. 1996. Adsorption of Organic Macromolecules by Granular Activated Carbon. 2. Influence of Dissolved Oxygen. Environ. Sci. Technol. 30(7), 2195-2201. https://doi.org/10.1021/es950587v

Kim, J., Kim, J. and Hong, S. 2018. Recovery of water and minerals from shale gas produced water by membrane distillation crystallization. Water Res. 129, 447-459. https://doi.org/10.1016/j.watres.2017.11.017

Lee, S., Sutter, M., Burkhardt, M., Wu, B. and Chong, T.H. 2019a. Biocarriers facilitated gravity-driven membrane (GDM) reactor for wastewater reclamation: Effect of intermittent aeration cycle. Sci. Total Environ. 694. https://doi.org/10.1016/j.scitotenv.2019.133719

Lee, S., Suwarno, S.R., Quek, B.W.H., Kim, L., Wu, B. and Chong, T.H. 2019b. A comparison of gravity-driven membrane (GDM) reactor and biofiltration + GDM reactor for seawater reverse osmosis desalination pretreatment. Water Res. 154, 72-83. https://doi.org/10.1016/j.watres.2019.01.044

Li, J., Chang, H., Tang, P., Shang, W., He, Q. and Liu, B. 2020. Effects of membrane property and hydrostatic pressure on the performance of gravity-driven membrane for shale gas flowback and produced water treatment. J. Water Process Eng. 33, 101117. https://doi.org/10.1016/j.jwpe.2019.101117

Liu, C., Song, D., Zhang, W., He, Q., Huangfu, X., Sun, S., Sun, Z., Cheng, W. and Ma, J. 2020. Constructing zwitterionic polymer brush layer to enhance gravity-driven membrane performance by governing biofilm formation. Water Res. 168, 115181. https://doi.org/10.1016/j.watres.2019.115181

Miller, D.J., Huang, X., Li, H., Kasemset, S., Lee, A., Agnihotri, D., Hayes, T., Paul, D.R. and Freeman, B.D. 2013. Fouling-resistant membranes for the treatment of flowback water from hydraulic shale fracturing: A pilot study. J. Membr. Sci. 437, 265-275. https://doi.org/10.1016/j.memsci.2013.03.019

Peter-Varbanets, M., Hammes, F., Vital, M. and Pronk, W. 2010. Stabilization of flux during dead-end ultra-low pressure ultrafiltration. Water Res. 44(12), 3607-3616. https://doi.org/10.1016/j.watres.2010.04.020

Peter-Varbanets, M., Margot, J., Traber, J. and Pronk, W. 2011. Mechanisms of membrane fouling during ultra-low pressure ultrafiltration. J. Membr. Sci. 377(1-2), 42-53. https://doi.org/10.1016/j.memsci.2011.03.029

Pronk, W., Ding, A., Morgenroth, E., Derlon, N., Desmond, P., Burkhardt, M., Wu, B. and Fane, A.G. 2019. Gravity-driven membrane filtration for water and wastewater treatment: A review. Water Res. 149, 553-565. https://doi.org/10.1016/j.watres.2018.11.062

Riley, S.M., Oliveira, J.M.S., Regnery, J. and Cath, T.Y. 2016. Hybrid membrane

bio-systems for sustainable treatment of oil and gas produced water and fracturing flowback water. Sep. Purif. Technol. 171, 297-311. https://doi.org/10.1016/j.seppur.2016.07.008

Shaffer, D.L., Arias Chavez, L.H., Ben-Sasson, M., Romero-Vargas Castrillón, S., Yip, N.Y. and Elimelech, M. 2013. Desalination and Reuse of High-Salinity Shale Gas Produced Water: Drivers, Technologies, and Future Directions. Environ. Sci. Technol. 47(17), 9569-9583. https://doi.org/10.1021/es401966e

Shang, W., Tiraferri, A., He, Q., Li, N., Chang, H., Liu, C. and Liu, B. 2019. Reuse of shale gas flowback and produced water: Effects of coagulation and adsorption on ultrafiltration, reverse osmosis combined process. Sci. Total Environ. 689, 47-56. https://doi.org/10.1016/j.scitotenv.2019.06.365

Shao, S., Feng, Y., Yu, H., Li, J., Li, G. and Liang, H. 2017. Presence of an adsorbent cake layer improves the performance of gravity-driven membrane (GDM) filtration system. Water Res. 108, 240-249. https://doi.org/10.1016/j.watres.2016.10.081

Shao, S., Shi, D., Li, Y., Liu, Y., Lu, Z., Fang, Z. and Liang, H. 2019. Effects of water temperature and light intensity on the performance of gravity-driven membrane system. Chemosphere 216, 324-330. https://doi.org/10.1016/j.chemosphere.2018.10.156

Shi, D., Liu, Y., Fu, W.W., Li, J.Y., Fang, Z. and Shao, S.L. 2020. A combination of membrane relaxation and shear stress significantly improve the flux of gravity-driven membrane system. Water Res. 175. https://doi.org/10.1016/j.watres.2020.115694

Song, D., Zhang, W., Cheng, W., Jia, B., Wang, P., Sun, Z., Ma, J., Zhai, X., Qi, J. and Liu, C. 2020a. Micro fine particles deposition on gravity-driven ultrafiltration membrane to modify the surface properties and biofilm compositions: Water quality improvement and biofouling mitigation. Chem. Eng. J. 393, 123270. https://doi.org/10.1016/j.cej.2019.123270

Song, J., Zhang, W., Gao, J., Hu, X., Zhang, C., He, Q., Yang, F., Wang, H., Wang, X. and Zhan, X. 2020b. A pilot-scale study on the treatment of landfill leachate by a composite biological system under low dissolved oxygen conditions: Performance and microbial community. Bioresour. Technol. 296, 122344. https://doi.org/10.1016/j.biortech.2019.122344

Tang, P., Liu, B., Zhang, Y., Chang, H., Zhou, P., Feng, M. and Sharma, V.K. 2020a. Sustainable reuse of shale gas wastewater by pre-ozonation with ultrafiltration-reverse osmosis. Chem. Eng. J. 392, 123743. https://doi.org/10.1016/j.cej.2019.123743

Tang, X., Cheng, X., Zhu, X., Xie, B., Guo, Y., Wang, J., Ding, A., Li, G. and Liang, H. 2018a. Ultra-low pressure membrane-based bio-purification process for decentralized drinking water supply: Improved permeability and removal performance. Chemosphere 211, 784-793. https://doi.org/10.1016/j.chemosphere.2018.07.183

Tang, X., Ding, A., Pronk, W., Ziemba, C., Cheng, X., Wang, J., Xing, J., Xie, B., Li, G. and Liang, H. 2018b. Biological pre-treatments enhance gravity-driven membrane filtration for the decentralized water supply: Linking extracellular polymeric substances formation to flux stabilization. J. Clean. Prod. 197, 721-731. https://doi.org/10.1016/j.jclepro.2018.06.155

585 Tang, X., Xie, B., Chen, R., Wang, J., Huang, K., Zhu, X., Li, G. and Liang, H. 2020b.
586 Gravity-driven membrane filtration treating manganese-contaminated surface water: Flux
587 stabilization and removal performance. Chem. Eng. J. 397, 125248.
588 https://doi.org/10.1016/j.cej.2020.125248
589 Tang, X.B., Pronk, W., Ding, A., Cheng, X.X., Wang, J.L., Xie, B.H., Li, G.B. and Liang, H.
590 2018c. Coupling GAC to ultra-low-pressure filtration to modify the biofouling layer and
591 bio-community: Flux enhancement and water quality improvement. Chem. Eng. J. 333,
592 289-299. https://doi.org/10.1016/j.cej.2017.09.111
593 Tong, T., Carlson, K.H., Robbins, C.A., Zhang, Z. and Du, X. 2019. Membrane-based
594 treatment of shale oil and gas wastewater: The current state of knowledge. Front. Env. Sci.
595 Eng. 13(4), 63. https://doi.org/10.1016/j.watres.2020.115694
596 Truttmann, L., Su, Y., Lee, S., Burkhardt, M., Brynjólfsson, S., Chong, T.H. and Wu, B. 2020.
597 Gravity-driven membrane (GDM) filtration of algae-polluted surface water. J. Water
598 Process Eng. 36, 101257. https://doi.org/10.1016/j.jwpe.2020.101257
599 Wang, H., Lu, L., Chen, X., Bian, Y. and Ren, Z.J. 2019. Geochemical and microbial
600 characterizations of flowback and produced water in three shale oil and gas plays in the
601 central and western United States. Water Res. 164, 114942.
602 https://doi.org/10.1016/j.watres.2019.114942
603 Wang, Y.R., Fortunato, L., Jeong, S. and Leiknes, T. 2017. Gravity-driven membrane system
604 for secondary wastewater effluent treatment: Filtration performance and fouling
605 characterization. Sep. Purif. Technol. 184, 26-33.
606 https://doi.org/10.1016/j.seppur.2017.04.027
607 Wu, B., Hochstrasser, F., Akhondi, E., Ambauen, N., Tschirren, L., Burkhardt, M., Fane, A.G.
608 and Pronk, W. 2016. Optimization of gravity-driven membrane (GDM) filtration
609 process for seawater pretreatment. Water Res. 93, 133-140.
610 https://doi.org/10.1016/j.watres.2016.02.021
611 Wu, B., Soon, G.Q.Y. and Chong, T.H. 2019. Recycling rainwater by submerged
612 gravity-driven membrane (GDM) reactors: Effect of hydraulic retention time and periodic
613 backwash. Sci. Total Environ. 654, 10-18. https://doi.org/10.1016/j.scitotenv.2018.11.068
614 Wu, B., Suwarno, S.R., Tan, H.S., Kim, L.H., Hochstrasser, F., Chong, T.H., Burkhardt, M.,
615 Pronk, W. and Fane, A.G. 2017. Gravity-driven microfiltration pretreatment for reverse
616 osmosis (RO) seawater desalination: Microbial community characterization and RO
617 performance. Desalination 418, 1-8. https://doi.org/10.1016/j.desal.2017.05.024
618 Xing, W., Ngo, H.H., Kim, S.H., Guo, W.S. and Hagare, P. 2008. Adsorption and
619 bioadsorption of granular activated carbon (GAC) for dissolved organic carbon (DOC)
620 removal in wastewater. Bioresour. Technol. 99(18), 8674-8678.
621 https://doi.org/10.1016/j.biortech.2008.04.012
622 Zhang, Y., Yu, Z., Zhang, H. and Thompson, I.P. 2017. Microbial distribution and variation
623 in produced water from separators to storage tanks of shale gas wells in Sichuan Basin,
624 China. Environ. Sci. Water Res. Technol. 3(2), 340-351.
625 https://doi.org/10.1039/C6EW00286B
626 Zou, C., Ni, Y., Li, J., Kondash, A., Coyte, R., Lauer, N., Cui, H., Liao, F. and Vengosh, A.

2018. The water footprint of hydraulic fracturing in Sichuan Basin, China. Sci. Total Environ. 630, 349-356. https://doi.org/10.1016/j.scitotenv.2018.02.219